COMPUTED TOMOGRAPHY

Glenoid bone loss in anterior shoulder dislocation: a multicentric study to assess the most reliable imaging method

Marcello Zappia[1,2,3] · Domenico Albano[4] · Alberto Aliprandi[5] · Antonio Barile[6] · Luca Brunese[1] ·
Alessandro Castagna[7,8] · Andrea Cozzolino[9] · Massimo De Filippo[10] · Francesco Di Pietto[11] ·
Mariano Giuseppe Di Salvatore[1] · Eugenio Annibale Genovese[12,13] · Salvatore Guarino[14] · Pasquale Guerriero[1] ·
Giovanni Merolla[15,16,17] · Carmelo Messina[4] · Riccardo Ranieri[8] · Alfonso Maria Romano[18] · Raffaele Russo[1,19] ·
Michele Tumminello[20] · Pierluigi Salvo Rossi[21] · Luca Maria Sconfienza[4,22] · Vito Chianca[23,24]

Abstract

Purpose The aim of this multicentric study was to assess which imaging method has the best inter-reader agreement for glenoid bone loss quantification in anterior shoulder instability. A further aim was to calculate the inter-method agreement comparing bilateral CT with unilateral CT and MR arthrography (MRA) with CT measurements. Finally, calculations were carried out to find the least time-consuming method.

Method A retrospective evaluation was performed by 9 readers (or pairs of readers) on a consecutive series of 110 patients with MRA and bilateral shoulder CT. Each reader was asked to calculate the glenoid bone loss of all patients using the following methods: best fit circle area on both MRA and CT images, maximum transverse glenoid width on MRA and CT, CT PICO technique, ratio of the maximum glenoid width to height on MRA and CT, and length of flattening of the anterior glenoid curvature on MRA and CT. Using Pearson's correlation coefficient (PCC), the following agreement values were calculated: the inter-reader for each method, the inter-method for MRA with CT quantifications and the inter-method for CT best-fit circle area and CT PICO. Statistical analysis was carried out to compare the time employed by the readers for each method.

Results Inter-reader agreement PCC mean values were the following: 0.70 for MRA and 0.77 for CT using best fit circle diameter, 0.68 for MRA and 0.72 for CT using best fit circle area, 0.75 for CT PICO, 0.64 for MRA and 0.62 for CT anterior straight line and 0.49 for MRA and 0.43 for CT using length-to-width ratio. CT-MRA inter-modality PCC mean values were 0.9 for best fit circle diameter, 0.9 for best fit circle area, 0.62 for anterior straight line and 0.94 for length-to-width methods. PCC mean value comparing unilateral CT with PICO CT methods was 0.8. MRA best fit circle area method was significantly faster than the same method performed on CT ($p = 0.031$), while no significant difference was seen between CT and MRA for remaining measurements.

Conclusions CT PICO is the most reliable imaging method, but both CT and MRA can be reliably used to assess glenoid bone loss. Best fit circle area CT and MRA methods are valuable alternative measurement techniques.

Keywords Anterior shoulder instability · Glenoid bony defect · Bone loss · Measurement technique · CT · MRI · PICO

Introduction

Recurrent anterior dislocation of the humeral head causes wear, remodelling and bone loss of the antero-inferior margin of glenoid [1]. The reduction of the glenohumeral contact area can further increase joint instability, thus causing failure in soft tissue-only surgery [2, 3]. Therefore, pre-operative knowledge of glenoid bone loss is important in choosing the best surgical approach, in other words, whether to perform capsulolabral repair alone or also bone augmentation (i.e., Latarjet procedure, open or arthroscopic bone block) [1, 4]. Different glenoid bone loss threshold values have been reported, ranging from 10 to 25% [5]. A recent expert consensus statement stated that bone graft reconstruction should be considered when the glenoid bone deficit is greater than 20% [6].

✉ Vito Chianca
vitochianca@gmail.com

Extended author information available on the last page of the article

Computed tomography (CT) was the first imaging modality to be used to assess glenoid bone loss: anterior glenoid flattening, decreased maximum glenoid width, and decreased maximum width-to-length ratio resulted the most useful parameters [7]. Later, PICO method was proposed to quantify the bone loss using the unaffected contralateral glenoid as a reference [8]. Then, the CT method was validated through arthroscopic comparison and magnetic resonance imaging (MRI) was also proposed as a valuable radiation-free alternative modality that demonstrates similar accuracy levels [9, 10]. The quantification of glenoid bone loss is still open to debate with regard to the radiological inter-reader discrepancy, the accuracy of MRI compared to CT, and the time-consuming processes of CT and MRI methods. Furthermore, nowadays because of the widespread use of both MR arthrography (MRA) to assess soft tissues and PICO method, acquiring CT images of both shoulders to assess glenoid bone loss, concerns have been raised regarding the economic impact on healthcare systems and radiation burden for patients.

In this context, the purpose of this multicentric study is to evaluate which method is the most easily reproduced and to establish agreement in the measurements carried out on CT and MRA and on unilateral and bilateral glenoid. According to our knowledge, there are no further multicentric and multi-reader studies in the literature that have compared different CT and MRA methods on a large sample of patients.

Material and methods

Study design

Campolongo Hospital Institutional review board approval was obtained. All participants of this study provided written informed consent for collection of data in order to use them for scientific purposes.

Patients

This study is concerned with the evaluation of a consecutive series of 110 patients with history of anterior shoulder dislocation who underwent shoulder MRA and unenhanced bilateral shoulder CT between January 2012 and April 2019 in three different hospitals (Campolongo Hospital, Medicanova Institute, Varelli Institute). All patients underwent both MRA and bilateral CT of the shoulder on the same day. Four patients were discarded, three of them for previous Latarjet surgery and one due to low quality MRA images related to motion artifacts. Six patients with bilateral glenoid bone deficiency were also

excluded. Finally, a total of 100 patients (86 males, 14 females; mean age: 26.4 ± 8.7 years, range 16–52) were included in the study.

MRA and CT examination technique

All MRA were performed on a 1.5 T magnet (Siemens Magnetom Aera, Toshiba Titan, and Philips® Achieva). MRA protocol included at least a Turbo spin-echo (TSE) T1-weighted sequence on the oblique sagittal plane with a maximum field of view (FOV) of 18 cm and a maximum slice thickness of 4 mm. Any volumetric sequences have been deleted from the dicom folder, thus using only the acquired oblique sagittal plane in measurements. DOTAREM® 0.0025 mmol/ml was injected as the intra-articular contrast agent.

Simultaneous CT examination of both shoulders was performed on two different CT scanners (Toshiba Aquilion 16; Aquilion 64) using a maximum FOV of 18 cm and $\leq 1{:}1.75$ pitch. The CT scanning plane extended from the acromion to just below the glenoid, with the patient's arms positioned along the chest wall and the palms pronated. In order to test the reader's variability in reconstructing the planes, only the native axial images were archived, and not the series of multiplanar reconstructed images.

MRA and CT analysis

All DICOM files were anonymized, renamed, and sent to 8 radiologists (2–30 years of musculoskeletal radiology experience) and 3 orthopedic surgeons (1–30 years of shoulder surgery experience). Of the latter, two of the orthopedists performed the calculations together with the reference radiologist, as would be done in clinical practice. Independently and blinded to clinical data, each reader or pair of readers (radiologist-orthopedic) calculated the glenoid bone loss of each patient using the following methods: best fit circle area on both MRA and CT images [10, 11] (Fig. 1a, b), maximum transverse glenoid width relative to diameter of best-fit circle on MRA and CT [10] (Fig. 2a, b), CT PICO technique [8] (Fig. 3a, b), ratio of the maximum glenoid fossa width to the maximum glenoid height on MRA and CT [7] (Fig. 4a, b) and length of flattening of the anterior glenoid curvature on MRA and CT [7] (Fig. 5a, b).

All readers were free to use the processing software of their choice to visualize the DICOM files and to perform all measurements. They were also asked to calculate the time taken for each of the measurements performed on the 20th patient.

Fig. 1 Turbo spin-echo T1-weighted **a** and CT **b** oblique images en face to glenoid. Glenoid bone loss is measured within best-fit circle. Glenoid bone loss is percentage reduction in osseous defect area (area y) relative to area of best-fit circle (area y + area x)
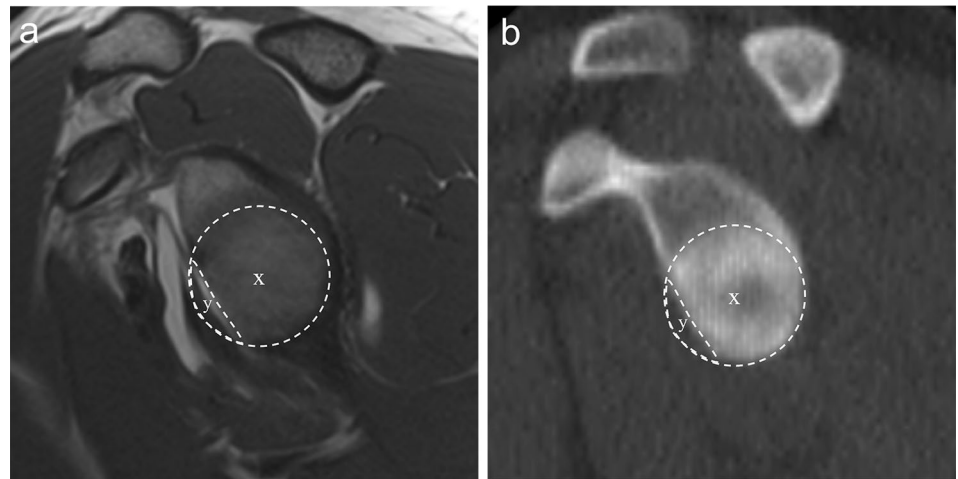
Fig. 2 Turbo spin-echo T1-weighted **a** and CT **b** oblique images en face to glenoid. Maximum transverse width of the bony glenoid (black line) is compared with diameter of best-fit circle (black + white line). Glenoid bone loss is percentage reduction in maximum transverse glenoid width relative to diameter of best-fit circle
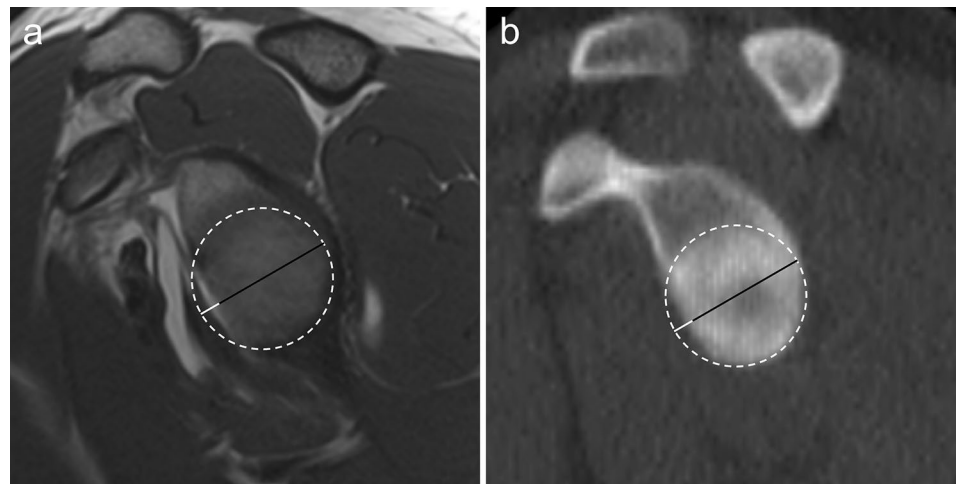
Fig. 3 PICO method. CT oblique reformatted images en face to glenoid of nondislocating **a** and dislocating shoulder **b**. Glenoid bone loss is percentage reduction in osseous defect area (area y) relative to area of best-fit circle drawn on nondislocating shoulder (area x, left)
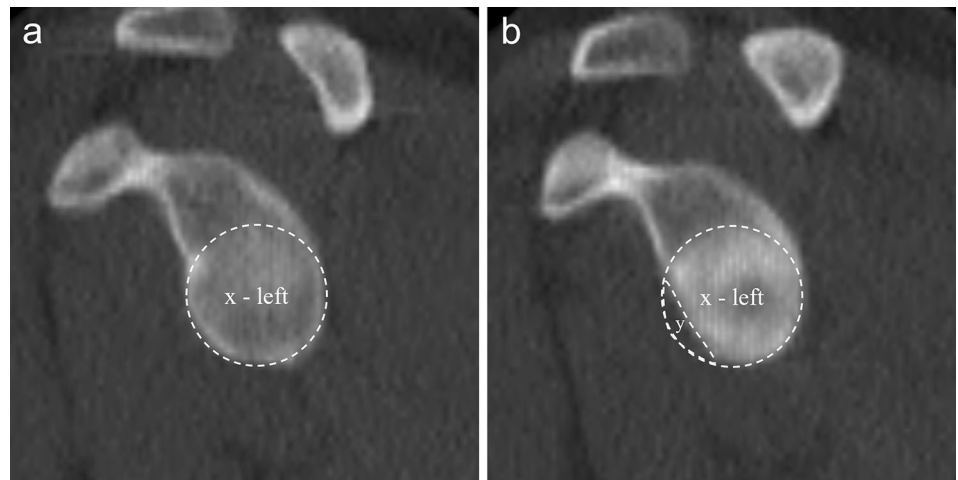
Data analysis

Statistical analysis was performed using MATLAB software (version R2020b). Data were preliminary processed to be expressed in common units. We used the Pearson's Correlation Coefficient (PCC) to calculate: (i) the inter-reader agreement for each quantification method; (ii) the intra-reader inter-modality agreement between MRA and CT using the best fit circle area, maximum transverse glenoid width relative to diameter of best-fit circle, ratio of

Fig. 4 Turbo spin-echo T1-weighted **a** and CT **b** oblique images en face to glenoid. Glenoid bone loss is measured as ratio of the maximum glenoid fossa width to the maximum glenoid height
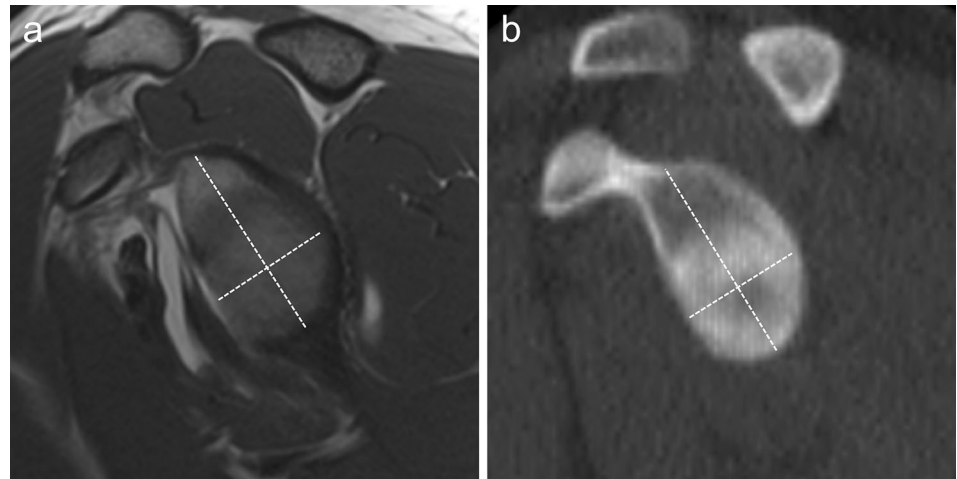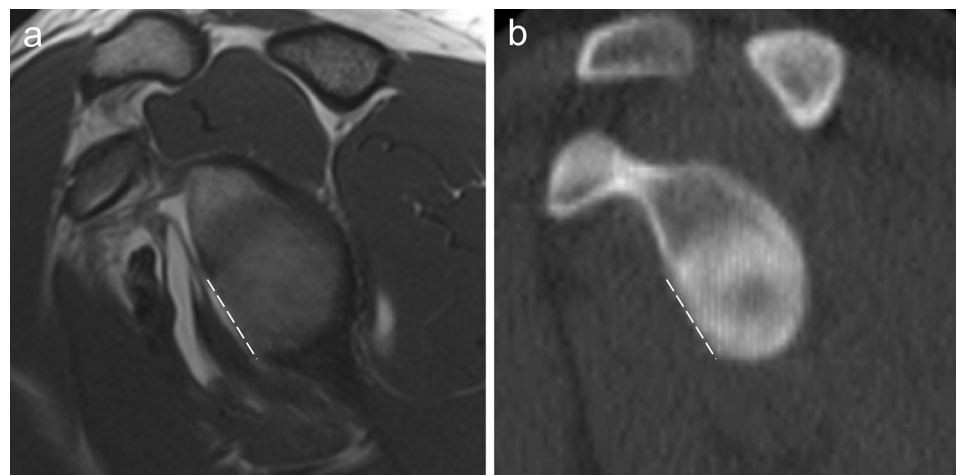

Fig. 5 Turbo spin-echo T1-weighted **a** and CT **b** oblique images en face to glenoid. Glenoid bone loss is measured as length of flattening of the anterior glenoid curvature (dashed line)

the maximum glenoid fossa width to the maximum glenoid height, and length of flattening of the anterior glenoid curvature; and (iii) the inter-modality agreement of bone loss area calculated with CT "best-fit circle" on unilateral glenoid and CT PICO method. The sequence index when computing PCCs is related to the patients and indices where at least one of the sequences had a missing value are deleted. The mean inter-reader discrepancy for each method was calculated, and the maximum error value was reported. Finally, the Mann–Whitney test was used to compare the time needed by the readers for bone loss quantification for each CT and MRA method. A p value < 0.05 was considered statistically significant.

Results

All inter-reader agreement PCC values are reported in Table 1. Inter-reader agreement PCC mean values were the following: 0.77 ± 0.08 (range 0.61–0.91) for CT best fit circle diameter; 0.72 ± 0.13 (0.35–0.91) for CT best fit circle area;

0.75 ± 0.10 (0.5–0.91) for CT PICO; 0.62 ± 0.1 (0.34–0.90) for CT anterior straight line; 0.43 ± 0.32 (0.15–0.86) for CT length-to-width ratio; 0.70 ± 0.1 (0.40–0.87) for MRA best fit circle diameter; 0.68 ± 0.13 (0.49–0.88) for MRA best fit circle area; 0.64 ± 0.11 (0.43–0.92), for MRA anterior straight line; 0.49 ± 0.22 (0.03–0.84) for MRA length-to-width ratio.

All inter-modality agreement PCC values are reported in Table 2.

For inter-modality agreement, the PCC mean value was 0.9 ± 0.1 ranging from 0.68 to 1.00 when comparing CT and MRA best fit circle diameter, 0.9 ± 0.1 with 0.68–0.97 range when comparing CT and MRA best fit circle area, 0.62 ± 0.33 with 0.07–0.93 range when comparing CT and MRA anterior straight line, and 0.94 ± 0.06 with 0.80–0.99 range when comparing CT and MRA length-to-width methods.

When comparing unilateral (best fit circle area) and bilateral glenoid bone loss (PICO) CT methods, the PCC mean value was 0.8 ± 0.2, ranging from 0.51 to 1.00.

These results are summarized in Figs. 6 and 7.

Table 1 Heatmap table shows the inter-reader agreement PCC values. The pair of readers are reported on the rows
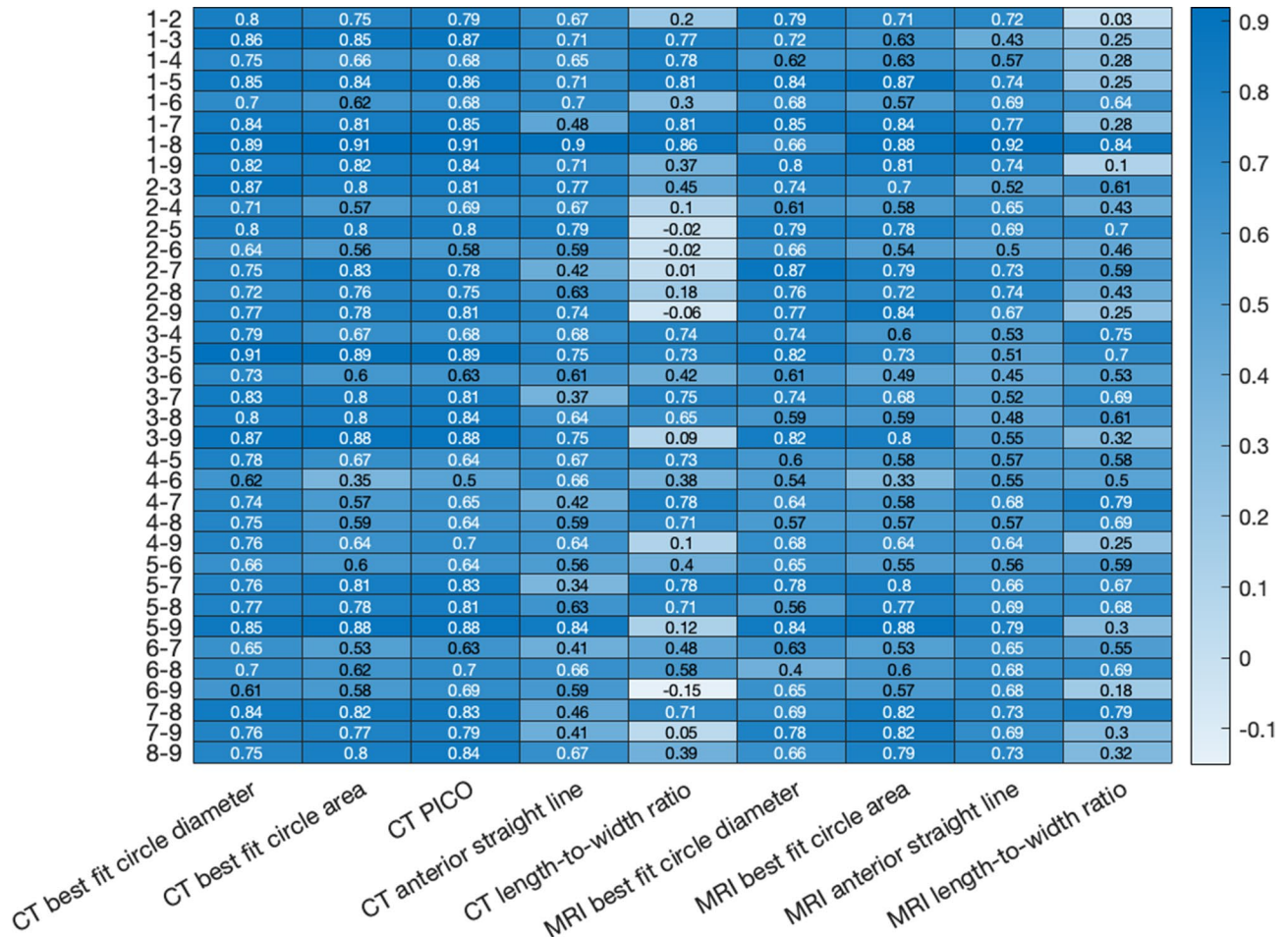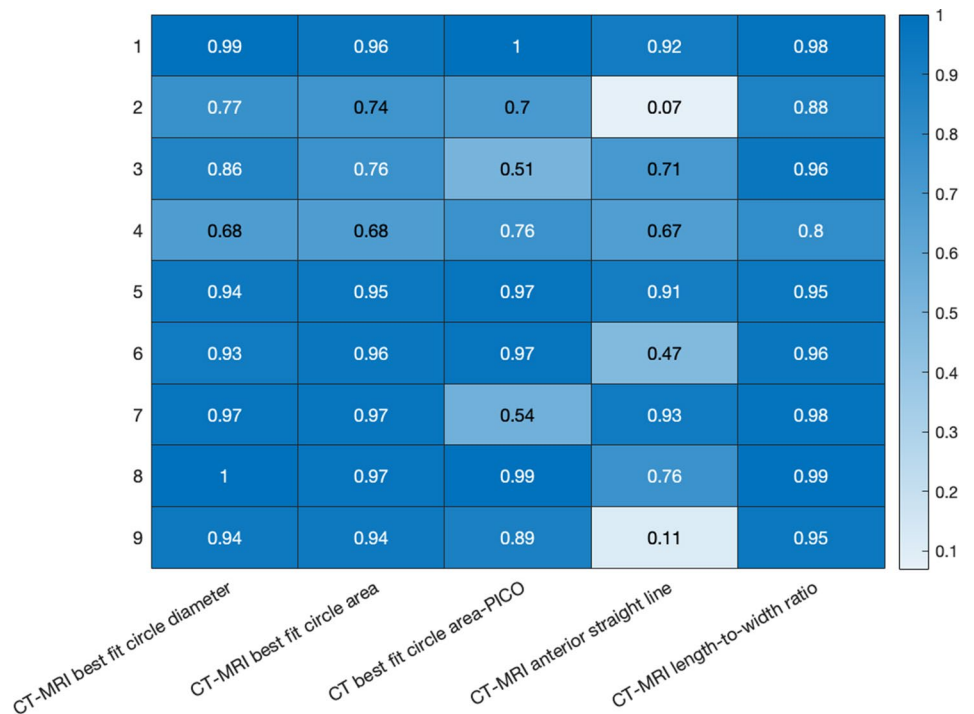
	CT best fit circle diameter	CT best fit circle area	CT PICO	CT anterior straight line	CT length-to-width ratio	MRI best fit circle diameter	MRI best fit circle area	MRI anterior straight line	MRI length-to-width ratio
1-2	0.8	0.75	0.79	0.67	0.2	0.79	0.71	0.72	0.03
1-3	0.86	0.85	0.87	0.71	0.77	0.72	0.63	0.43	0.25
1-4	0.75	0.66	0.68	0.65	0.78	0.62	0.63	0.57	0.28
1-5	0.85	0.84	0.86	0.71	0.81	0.84	0.87	0.74	0.25
1-6	0.7	0.62	0.68	0.7	0.3	0.68	0.57	0.69	0.64
1-7	0.84	0.81	0.85	0.48	0.81	0.85	0.84	0.77	0.28
1-8	0.89	0.91	0.91	0.9	0.86	0.66	0.88	0.92	0.84
1-9	0.82	0.82	0.84	0.71	0.37	0.8	0.81	0.74	0.1
2-3	0.87	0.8	0.81	0.77	0.45	0.74	0.7	0.52	0.61
2-4	0.71	0.57	0.69	0.67	0.1	0.61	0.58	0.65	0.43
2-5	0.8	0.8	0.8	0.79	-0.02	0.79	0.78	0.69	0.7
2-6	0.64	0.56	0.58	0.59	-0.02	0.66	0.54	0.5	0.46
2-7	0.75	0.83	0.78	0.42	0.01	0.87	0.79	0.73	0.59
2-8	0.72	0.76	0.75	0.63	0.18	0.76	0.72	0.74	0.43
2-9	0.77	0.78	0.81	0.74	-0.06	0.77	0.84	0.67	0.25
3-4	0.79	0.67	0.68	0.68	0.74	0.74	0.6	0.53	0.75
3-5	0.91	0.89	0.89	0.75	0.73	0.82	0.73	0.51	0.7
3-6	0.73	0.6	0.63	0.61	0.42	0.61	0.49	0.45	0.53
3-7	0.83	0.8	0.81	0.37	0.75	0.74	0.68	0.52	0.69
3-8	0.8	0.8	0.84	0.64	0.65	0.59	0.59	0.48	0.61
3-9	0.87	0.88	0.88	0.75	0.09	0.82	0.8	0.55	0.32
4-5	0.78	0.67	0.64	0.67	0.73	0.6	0.58	0.57	0.58
4-6	0.62	0.35	0.5	0.66	0.38	0.54	0.33	0.55	0.5
4-7	0.74	0.57	0.65	0.42	0.78	0.64	0.58	0.68	0.79
4-8	0.75	0.59	0.64	0.59	0.71	0.57	0.57	0.57	0.69
4-9	0.76	0.64	0.7	0.64	0.1	0.68	0.64	0.64	0.25
5-6	0.66	0.6	0.64	0.56	0.4	0.65	0.55	0.56	0.59
5-7	0.76	0.81	0.83	0.34	0.78	0.78	0.8	0.66	0.67
5-8	0.77	0.78	0.81	0.63	0.71	0.56	0.77	0.69	0.68
5-9	0.85	0.88	0.88	0.84	0.12	0.84	0.88	0.79	0.3
6-7	0.65	0.53	0.63	0.41	0.48	0.63	0.53	0.65	0.55
6-8	0.7	0.62	0.7	0.66	0.58	0.4	0.6	0.68	0.69
6-9	0.61	0.58	0.69	0.59	-0.15	0.65	0.57	0.68	0.18
7-8	0.84	0.82	0.83	0.46	0.71	0.69	0.82	0.73	0.79
7-9	0.76	0.77	0.79	0.41	0.05	0.78	0.82	0.69	0.3
8-9	0.75	0.8	0.84	0.67	0.39	0.66	0.79	0.73	0.32

Table 2 Heatmap table shows the inter-modality agreement PCC values. The readers are reported on the rows

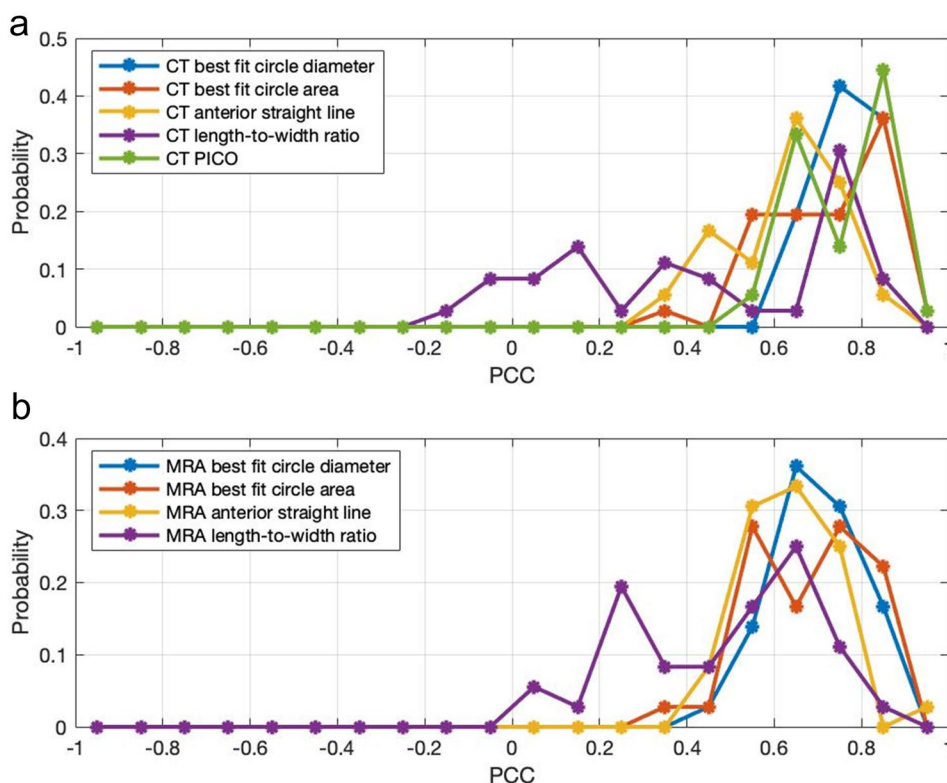|	CT-MRI best fit circle diameter	CT-MRI best fit circle area	CT best fit circle area-PICO	CT-MRI anterior straight line	CT-MRI length-to-width ratio
1	0.99	0.96	1	0.92	0.98
2	0.77	0.74	0.7	0.07	0.88
3	0.86	0.76	0.51	0.71	0.96
4	0.68	0.68	0.76	0.67	0.8
5	0.94	0.95	0.97	0.91	0.95
6	0.93	0.96	0.97	0.47	0.96
7	0.97	0.97	0.54	0.93	0.98
8	1	0.97	0.99	0.76	0.99
9	0.94	0.94	0.89	0.11	0.95

Fig. 6 Inter-reader agreement analysis. The results of inter-reader agreement analysis via normalized histograms of the fraction of reader's pairs having a given level of agreement (measured in terms of PCC) when basing their assessments on a specific feature. The results are split in two subfigures for ease of reading, dividing the results related to CT **A** and MRA **B**. As an example, the second rightmost point of the green curve on the upper subfigure denotes that approximately 45% of the surgeon's pair have high level of agreement (PCC close to 0.9) when basing their assessments on CT PICO. An appar-ent information extracted from the inter-reader agreement results is that the green curve is the one exhibiting its peaks toward the right side (closer to PCC = 1); then blue, red and yellow curves follow; and finally, the purple curves have their peaks toward the center (closer to PCC = 0). This means that reader shows higher level of agreement when basing their assessments on CT PICO (resp. length-to-width ratio), while the level of agreement is intermediate when based on the remaining imaging features. This behavior is confirmed for both CT-based and MRI-based features

The lowest level of inter-reader discrepancy was seen in CT PICO technique (4.16%), followed by CT and MRA best fit circle area methods (both 4.67%). Mean inter-reader discrepancy results are reported in Table 3.

The average time taken by each reader for each method ranges from 31.33 s for MRA anterior straight line to 102.00 s for PICO technique (see Table 4). MRA best fit circle area method was significantly faster than the same method performed on CT ($p = 0.031$), while no significant difference was seen in CT/MRA best fit circle diameter ($p = 0.666$), CT/MRA anterior straight line ($p = 0.340$), and CT/MRA length-to-width methods ($p = 0.730$).

Discussion

The main finding of this study is that CT PICO is the method with the highest inter-reader agreement and the lowest mean value of discrepancy in terms of glenoid bone loss percentage. Similarly, the calculation of the area and diameter with the best fit circle method in both MRA and CT also showed high inter-reader agreement. Furthermore, the greatest level of inter-modality agreement was reached by the best fit circle area CT and the PICO CT, followed by CT/MRA best fit circle area and best fit circle diameter.

Several studies have applied different methods and imaging modalities in the evaluation of glenoid bone loss in patients with anterior shoulder dislocation history [7, 9, 12, 13]. In fact, despite the established negative impact of large bone defects on the surgical outcome of glenohumeral soft-tissue stabilization interventions, there is no consensus on the gold standard technique for correctly quantifying glenoid bone loss pre-operatively [14]. It must be noted that the various methods are not interchangeable, given that threshold values used for critical glenoid bone loss cannot be compared. Consequently, high variability has been reported in the use of diagnostic methods in clinical practice with no consensus on threshold values for glenoid bone loss in
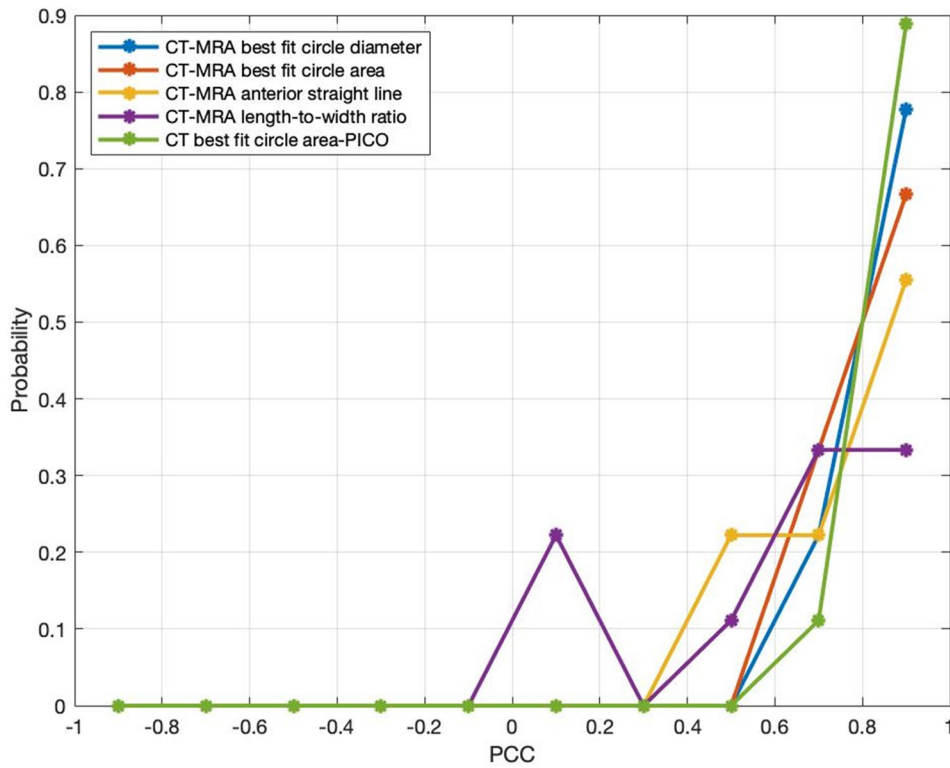
Fig. 7 Inter-modality agreement analysis. Results of the inter-modality agreement analysis via normalized histograms of the fraction of surgeons having a given level of agreement (measured in terms of PCC) when comparing their own assessments based on a pair of different-but-related bone loss quantification methods. As an example, the rightmost point of the purple curve on the figure denotes that approximately 35% of the readers have high level of agreement (PCC close to 0.9) when comparing their own assessments based on CT length-to-width ration and on MRI length-to-width ratio. An appar-

ent information extracted from the intra-reader agreement results is that the green curve is the one exhibiting its peak toward the right side (closer to PCC = 1), while the purple curve has its peaks toward the center (closer to PCC = 0). This means that surgeons show higher (resp. lower) level of agreement when comparing their assessments on best fit circle diameter (resp. length-to-width ratio), while the level of agreement is intermediate when based on the remaining pairs of clinical features

Table 3 Mean inter-reader discrepancy (MID) with standard deviation (SD) and maximum discrepancy (D-MAX) values are reported

	Mean discrepancy	STD	Max.
CT best fit circle diameter	5.41	4.94	30.70
CT best fit circle area	4.67	4.24	31.00
CT PICO	4.16	4.01	24.00
CT anterior straight line	6.09	8.10	31.80
CT length-to-width ratio	0.08	0.40	5.60
MRA best fit circle diameter	5.69	5.45	43.00
MRA best fit circle area	4.67	4.47	34.40
MRA anterior straight line	5.53	5.83	27.00
MRA length-to-width ratio	0.06	0.09	1.19

Table 4 Mean time to assess glenoid bone loss with different CT and MRA methods

	Seconds
CT best fit circle diameter	63
CT best fit circle area	102
CT PICO	102
CT anterior straight line	46
CT length-to-width ratio	53
MRA best fit circle diameter	68
MRA best fit circle area	80
MRA anterior straight line	31
MRA length-to-width ratio	55

surgical decision-making [15]. Hence, there has been an urgent request by the scientific community over recent decades for data from research studies regarding pre-operative imaging.

In this context, a reliable, reproducible, and easy-to-use imaging method for the assessment of glenoid bone loss is required for application in clinical practice. According to our data, CT PICO technique shows the greatest level of inter-reader agreement. In fact, CT is widely used to assess

glenoid bone loss, using multiplanar reconstructions to build en face sagittal images of the glenoid with clear cortical contours. Methods besides PICO have been proposed to measure glenoid bone loss with interesting results, such as the best fit circle area or diameter, ratio of the maximum glenoid fossa width-to-height, and length of flattening of the anterior glenoid [9, 12]. All these measurements have the strong advantage of being measured on a single shoulder CT, without the use of bilateral CT acquisition, thereby reducing radiation exposure [7]. In our study in particular, the best fit circle area method showed optimal inter-reader agreement values and high inter-method agreement values with PICO. Our results suggest that the acquisition of data from both shoulders is not mandatory for glenoid bone loss measurement. We also found that all these measurements—except for the best fit circle area—can be obtained faster than with the PICO method. One strength of PICO and best fit circle area methods, however, is that these are independent from the site and morphology of glenoid bone loss which, in turn, affects the other CT measurements of glenoid bone loss [16]. Nevertheless, it is worth nothing that a tracing tool, which is not available on all PACS systems, is required to calculate bone loss with PICO method, whereas the CT measurements performed on a single shoulder can be easily carried out with routinely available linear measuring tools.

It is interesting to note that three-dimensional CT is strongly supported by several studies which report it as an accurate, reliable tool for surgical planning [17]. The disadvantage, however, is that it requires post-processing and presents some limitations. Using a 3D image to calculate the area might increase the risk of mistakenly including portions of bone located medial to the articular plane in the measurement. What is more, some studies have reported low correlation between 3D CT and arthroscopy data [18]. However, it should be noted that, although arthroscopy has been used extensively as a reference standard in previous imaging studies, arthroscopy tends to overestimate glenoid bone loss using the bare spot method whose inaccuracy has been demonstrated [19]. Arthroscopic measurements of bone loss also rely on the bare area as an anatomic landmark for the glenoid central point, despite the fact that it can be absent and its position is extremely variable [20, 21]

MRI is increasing under scrutiny as a radiation-free alternative to CT in the assessment of glenoid bone loss [22, 23]. The rationale lies in the fact that patients with glenohumeral dislocation are routinely subjected to MRA to assess labrum, capsule-ligamentous, chondral, and rotator cuff injuries [24], while CT is performed only to evaluate bone status. According to our results, MRA measurements are reliable in this setting, demonstrating high inter-reader agreement, particularly with the best fit circle area and diameter methods which also show high agreement with CT measurements. This is in line with previous studies that

reported high inter-reader agreement values in evaluating glenoid bone loss on two-dimensional [22, 23] and three-dimensional MRI [25]. Moreover, MRI measurements have been shown to be accurate when compared with arthroscopy as reference standard [25, 26]. In this regard, it should be underlined that three-dimensional sequences are not always included in standard MRA protocols [27] and have the drawback of longer acquisition times. MRA measurements have the advantage of being slightly faster than those performed on CT, with a significant reduction of the time employed to calculate glenoid bone loss using MRA best fit circle area method, due to the immediate availability of sagittal images to perform all measurements and no need for multiplanar reconstructions. Furthermore, the recent introduction of Ultrashort echo time, Zero echo time and other CT-like bone contrast sequences promises further improvement in bone loss assessment [28–30].

This study has some limitations. First, only inter-reader and inter-methods agreement of these CT and MRA measurement were evaluated, while the clinical impact of these measurements on surgical decision-making, which was beyond the scope of the paper, was not tested. Neither was the use of three-dimensional CT images, but we believe that standardized surface measurements should be performed on multiplanar sagittal reconstructions of two-dimensional CT images. We did not evaluate operated patients. Finally, the time employed to perform all measurements may have been affected using different processing software to visualize the images.

In conclusion, both CT and MRA can be reliably used to assess glenoid bone loss in patients with a history of anterior shoulder dislocation. CT PICO is the most reliable imaging method, but other CT and MRA methods, particularly the best fit circle area, are valuable alternative measurement techniques that can be used to avoid the acquisition of data from both shoulders and limit pre-operative planning to the use of MRA only.

Declarations

Conflict of interest The authors declare that they have no conflict of interest.

Ethical Statement Ethical standards: this article does not contain any studies with human participants or animals performed by any of the authors.

References

1. Burkhart SS, De Beer JF (2000) Traumatic glenohumeral bone defects and their relationship to failure of arthroscopic Bankart

repairs: significance of the inverted-pear glenoid and the humeral engaging Hill-Sachs lesion. Arthrosc J Arthrosc Relat Surg 16:677–694

2. Boileau P, Villalba M, Héry J-Y et al (2006) Risk factors for recurrence of shoulder instability after arthroscopic Bankart repair. J Bone J Surg 88:1755–1763

3. Burkhart SS, DeBeer JF, Tehrany AM, Parten PM (2002) Quantifying glenoid bone loss arthroscopically in shoulder instability. Arthrosc J Arthrosc Relat Surg 18:488–491

4. Russo R, Maiotti M, Cozzolino A et al (2021) Arthroscopic iliac crest bone allograft combined with subscapularis upper-third tenodesis shows a low recurrence rate in the treatment of recurrent anterior shoulder instability associated with critical bone loss. Arthrosc J Arthrosc Relat Surg 37:824–833

5. Shin S-J, Koh YW, Bui C et al (2016) What is the critical value of glenoid bone loss at which soft tissue Bankart repair does not restore glenohumeral translation, restricts range of motion, and leads to abnormal humeral head position? Am J Sports Med 44:2784–2791

6. Rossi LA, Frank RM, Wilke D et al (2021) Evaluation and management of glenohumeral instability with associated bone loss: an expert consensus statement using the modified Delphi technique. Arthrosc J Arthrosc Relat Surg 37:1719–1728

7. Griffith JF, Antonio GE, Tong CWC, Ming CK (2003) Anterior shoulder dislocation: quantification of glenoid bone loss with CT. Am J Roentgenol 180:1423–1430

8. Baudi P, Campochiaro G, Rebuzzi M et al (2013) Assessment of bone defects in anterior shoulder instability. Joints 1:40

9. Griffith JF, Yung PSH, Antonio GE et al (2007) CT compared with arthroscopy in quantifying glenoid bone loss. Am J Roentgenol 189:1490–1493

10. Lee RKL, Griffith JF, Tong MMP et al (2013) Glenoid bone loss: assessment with MR imaging. Radiology 267:496–502

11. Huijsmans PE, Haen PS, Kidd M et al (2007) Quantification of a glenoid defect with three-dimensional computed tomography and magnetic resonance imaging: a cadaveric study. J Shoulder Elb Surg 16:803–809

12. De Filippo M, Castagna A, Steinbach LS et al (2013) Reproducible noninvasive method for evaluation of glenoid bone loss by multiplanar reconstruction curved computed tomographic imaging using a cadaveric model. Arthrosc J Arthrosc Relat Surg 29:471–477

13. Sugaya H (2014) Techniques to evaluate glenoid bone loss. Curr Rev Musculoskelet Med 7:1–5

14. Verweij LPE, Schuit AA, Kerkhoffs GMMJ et al (2020) Accuracy of currently available methods in quantifying anterior glenoid bone loss: controversy regarding gold standard—a systematic review. Arthrosc J Arthrosc Relat Surg 36:2295–2313

15. Weel H, Tromp W, Krekel PR et al (2016) International survey and surgeon's preferences in diagnostic work-up towards treatment of anterior shoulder instability. Arch Orthop Trauma Surg 136:741–746. https://doi.org/10.1007/S00402-016-2443-7

16. Altan E, Ozbaydar MU, Tonbul M, Yalcin L (2014) Comparison of two different measurement methods to determine glenoid bone defects: area or width? J Shoulder Elb Surg 23:1215–1222. https://doi.org/10.1016/J.JSE.2013.11.029

17. Saliken DJ, Bornes TD, Bouliane MJ et al (2015) Imaging methods for quantifying glenoid and Hill-Sachs bone loss in traumatic instability of the shoulder: a scoping review. BMC Musculoskelet Disord. https://doi.org/10.1186/S12891-015-0607-1

18. Walter WR, Samim M, LaPolla FWZ, Gyftopoulos S (2019) Imaging quantification of glenoid bone loss in patients with glenohumeral instability: a systematic review. Am J Roentgenol 212:1096–1105. https://doi.org/10.2214/AJR.18.20504

19. Bakshi NK, Patel I, Jacobson JA et al (2015) Comparison of 3-dimensional computed tomography-based measurement of glenoid bone loss with arthroscopic defect size estimation in patients with anterior shoulder instability. Arthroscopy 31:1880–1885. https://doi.org/10.1016/J.ARTHRO.2015.03.024

20. Kralinger F, Aigner F, Longato S et al (2006) Is the bare spot a consistent landmark for shoulder arthroscopy? A study of 20 embalmed glenoids with 3-dimensional computed tomographic reconstruction. Arthrosc J Arthrosc Relat Surg 22:428–432. https://doi.org/10.1016/J.ARTHRO.2005.12.006

21. Takeda Y, Miyatake K, Fujii K et al (2014) Validity of arthroscopic measurement of glenoid bone loss using the bare spot. Open Access J Sport Med 5:37. https://doi.org/10.2147/OAJSM.S58748

22. Gyftopoulos S, Hasan S, Bencardino J et al (2012) Diagnostic accuracy of MRI in the measurement of glenoid bone loss. Am J Roentgenol 199:873–878. https://doi.org/10.2214/AJR.11.7639

23. Stecco A, Guenzi E, Cascone T et al (2013) MRI can assess glenoid bone loss after shoulder luxation: inter- and intra-individual comparison with CT. Radiol Med 118:1335–1343. https://doi.org/10.1007/S11547-013-0927-X

24. Sconfienza LM, Albano D, Messina C et al (2018) How, when, why in magnetic resonance arthrography: an international survey by the European society of musculoskeletal radiology (ESSR). Eur Radiol 28:2356–2368. https://doi.org/10.1007/s00330-017-5208-y

25. Gyftopoulos S, Beltran LS, Yemin A et al (2014) Use of 3D MR reconstructions in the evaluation of glenoid bone loss: a clinical study. Skelet Radiol 43:213–218

26. Souza PM, Brandão BL, Brown E et al (2014) Recurrent anterior glenohumeral instability: the quantification of glenoid bone loss using magnetic resonance imaging. Skelet Radiol 43:1085–1092. https://doi.org/10.1007/S00256-014-1894-6

27. Bellelli A, Silvestri E, Barile A et al (2019) Position paper on magnetic resonance imaging protocols in the musculoskeletal system (excluding the spine) by the Italian College of Musculoskeletal Radiology. Radiol Med. https://doi.org/10.1007/s11547-019-00992-3

28. Lee K, Sim FY (2021) 3D MRI with CT-like bone contrast—an overview of current approaches and practical clinical implementation. Eur J Radiol 143:109915

29. Breighner RE, Endo Y, Konin GP et al (2018) Technical developments: zero echo time imaging of the shoulder: enhanced osseous detail by using MR imaging. Radiology 286:960–966

30. Lansdown DA, Pedoia V (2020) Editorial commentary: can we evaluate glenoid bone with magnetic resonance imaging? Yes, if you have the right sequence. Arthrosc J Arthrosc Relat Surg 36:2401–2402

Authors and Affiliations

Marcello Zappia[1,2,3] · Domenico Albano[4] · Alberto Aliprandi[5] · Antonio Barile[6] · Luca Brunese[1] · Alessandro Castagna[7,8] · Andrea Cozzolino[9] · Massimo De Filippo[10] · Francesco Di Pietto[11] · Mariano Giuseppe Di Salvatore[1] · Eugenio Annibale Genovese[12,13] · Salvatore Guarino[14] · Pasquale Guerriero[1] · Giovanni Merolla[15,16,17] · Carmelo Messina[4] · Riccardo Ranieri[8] · Alfonso Maria Romano[18] · Raffaele Russo[1,19] · Michele Tumminello[20] · Pierluigi Salvo Rossi[21] · Luca Maria Sconfienza[4,22] · Vito Chianca[23,24]

1   Department of Medicine and Health Sciences, University of Molise, Campobasso, Italy

2   Musculoskeletal Radiology Unit, Varelli Institute, Naples, Italy

3   Campolongo Hospital, Eboli, SA, Italy

4   IRCCS Istituto Ortopedico Galeazzi, Milan, Italy

5   Unit of Radiology, Clinical Institutes Zucchi, Monza, Monza Brianza, Italy

6   Department of Applied Clinical Sciences and Biotechnology, University of L'Aquila, 67100 L'Aquila, Italy

7   Humanitas Clinical and Research Center – IRCCS, Rozzano, MI, Italy

8   Department of Biomedical Sciences, Humanitas University, Pieve Emanuele, Milan, Italy

9   Department of Public Health, Division of Orthopaedic Surgery, Federico II'' University, Via S. Pansini 5, Bd. 12, 80131 Naples, Italy

10 University of Parma, Parma Hospital, Via Gramsci 14, 43126 Parma, Italy

11 Department of Radiology, Pineta Grande Hospital, Castel Volturno, CE, Italy

12 Insubria University, Varese, Italy

13 Intermedica-Columbus, Clinical Medical Center, Milan, Italy

14 Department of Radiology, Azienda Ospedaliera Dei Colli, Monaldi Hospital, Naples, Italy

15 Shoulder and Elbow Unit, Cervesi Hospital, AUSL Romagna, Cattolica, Italy

16 Doctorate School in Clinical and Experimental Medicine, UNIMORE, Modena, Italy

17 Upper Limb Surgery and Biomechanics Laboratory, AUSL Romagna, Ravenna, Italy

18 Department of Shoulder Surgery, Campolongo Hospital, Eboli, Italy

19 Second Orthopaedic and Traumatology Unit, Pineta Grande Hospital, Caserta, Italy

20 Department of Economics, Business, and Statistics, University of Palermo, Palermo, Italy

21 Department of Electronic Systems, Norwegian University of Science and Technology, Trondheim, Norway

22 Department of Biomedical Sciences for Health, University of Milano, Milan, Italy

23 Clinica Di Radiologia EOC IIMSI, Lugano, Switzerland

24 Ospedale Evangelico Betania, Via Argine 604, 80147 Naples, Italy